Histol Histopathol (2016) 31: 317-327

http://www.hh.um.es

Histology and Histopathology

From Cell Biology to Tissue Engineering

Immunocytochemical localization of the calcium-binding proteins calbindin D28K, calretinin and parvalbumin in bat visual cortex

Hang-Gu Kim[1], Ya-Nan Gu[1], Kyoung-Pil Lee[1], Ji-Gun Lee[1], Chan-Wook Kim[2], Ji-Won Lee[2], Tae-Hee Jeong[2], Young-Wun Jeong[2] and Chang-Jin Jeon[1]

[1]Department of Biology, School of Life Sciences, BK21 Plus KNU Creative BioResearch Group, College of Natural Sciences, and Brain Science and Engineering Institute, Kyungpook National University, Daegu and [2]Korea Science Academy of KAIST, Baegyanggwanmun-ro, Busanjin-gu, Busan, South Korea

Summary. It is a common misconception that bats are blind, and various studies have suggested that bats have visual abilities. The purpose of this study was to investigate the cytoarchitecture of calbindin D28K (CB)-, calretinin (CR)-, and parvalbumin (PV)-immunoreactive (IR) neurons in the bat visual cortex using immunocytochemistry. The highest density of CB- and PV-IR neurons was located in layer IV of the visual cortex. The majority of CB- and PV-IR neurons were characterized by a stellate or round/oval shape. CR-IR neurons were predominantly located in layers II/III, and the cells were principally round/oval in shape. Two-color immunofluorescence revealed that 65.96%, 24.24%, and 77.00% of the CB-, CR-, and PV-IR neurons, respectively, contained gamma-aminobutyric acid (GABA). We observed calcium-binding protein (CBP)-IR neurons in specific layers of the bat visual cortex and in specific cell types. Many of the CBP-IR neurons were GABAergic interneurons. These data provide useful clues to aid in understanding the functional aspects of the bat visual system.

Key words: Calbindin, Calretinin, Parvalbumin, Visual cortex, Immunocytochemistry

Offprint requests to: Prof. Chang-Jin Jeon, Neuroscience Lab., Department of Biology, College of Natural Sciences, Kyungpook National University, 80 Daehakro, Bukgu, Daegu, 41566, South Korea. e-mail: cjjeon@knu.ac.kr

DOI: 10.14670/HH-11-680

Introduction

It is a misconception that bats are blind and rely solely on echolocation rather than visual abilities to catch prey and monitor their surroundings (Simmons, 1973; Jones and Rayner, 1989). Bats have two eyes, and many of them rely on visual clues for sight, predation, and self-defense (Suthers and Wallis, 1970b; Vaughan and Vaughan, 1986). Bats are divided into two different suborders: *Megachiroptera* (megabats; about 200 species found throughout Asia, Africa, and Australasia) and *Microchiroptera* (microbats; about 800 species found throughout the world). Megabats, known as fruit bats and flying foxes, generally navigate by sight; they have large eyes and excellent eyesight (Suthers, 1970a; Holland et al., 2004). In contrast, microbats mostly rely on echolocation to fly; they have small eyes and poor eyesight (Neuweiler, 1990; Surlykke et al., 2009).

The greater horseshoe bat, *Rhinolophus ferrumequinum*, is a type of microbat. This species is cave-dwelling, insectivorous, and capable of echolocation (Jones and Rayner, 1989; Hage, 2013). Although microbats have tiny eyes that may be functional, their visual abilities and the functional organization of the central visual system are poorly understood (Jeon et al., 2007; Kim et al., 2008). Vision in microbats is based on several adaptations, such as the presence of functional opsin genes (Zhao et al., 2009; Xuan et al., 2012), utilization of ultraviolet light (Winter et al., 2003; Xuan et al., 2012), and use of light intensity

to detect and acquire food (Gutierrez et al., 2014).

Calcium-binding proteins (CBPs) are valuable markers for specific neuronal subpopulations in the central nervous system (CNS) (Baimbridge et al., 1992; Alexianu et al., 1994). Among these CBPs, calbindin D28K (CB), calretinin (CR), and parvalbumin (PV), the EF-hand calcium-binding proteins, are frequently expressed in neuronal cells (Baimbridge et al., 1992; Schäfer and Heizmann, 1996). CB is the prominent cytosolic vitamin D-dependent CBP in intestine and kidney (Welsh, 1988). CR is a neuron-specific CBP found in a distinct population of neurons in the brain, spinal cord, retina, and sensory ganglia. It shares about 58% homology with CB (Rogers, 1987; Ellis et al., 1991). PV was the first CBP to be isolated from the skeletal muscle of lower vertebrates, and has a molecular weight near 12,000 daltons (Da) (Heizmann, 1984; Heizmann et al., 1990). However, the functions of these CBPs are not yet fully established.

CB, CR, and PV were localized in the visual cortex of several mammals, including human (Blümcke et al., 1990; Leuba and Saini, 1996; Leuba et al., 1998), monkey (Blümcke et al., 1990; Hendrickson et al., 1991; Meskenaite, 1997; Glezer et al., 1998; Goodchild and Martin, 1998), dolphin (Glezer at al., 1992, 1998), cat (Stichel et al., 1987; Demeulemeester et al., 1991; Jeon and Park, 1997), rabbit (Park et al., 2000), flying fox (Ichida et al., 2000), ferret (Gao et al., 2000), rat (Gonchar and Burkhar, 1997), mouse (Park et al., 1999; Park et al., 2002), and hamster (Park et al., 1999; Lee et al., 2004). However, the distribution and morphology of CBP-immunoreactive (IR) neurons have not been studied in the bat visual cortex. Thus, the present study was undertaken to determine the laminar distribution and morphology of these three types of CBP-IR neurons in the bat visual cortex and to compare our results with other species. We also investigated whether the CBP-IR neurons in the bat visual cortex were gamma-aminobutyric acid (GABA)-ergic interneurons. Moreover, this study was a part of a large effort in our laboratory to localize CBPs in the entire bat visual system (Gonchar and Burkhalter, 1997; Jeon et al., 2007; Jeong et al., 2014).

Materials and methods

Perfusion and tissue processing

For this study, a total of 10 freshly caught adult bats (*Rhinolophus ferrumequinum*, both sexes: 15-20 g) were used. All bats were captured in a cave in the district of Milyang, South Korea. A net trap was used to catch the bats and the bats were transferred within one to two hours to the animal facility at the Neuroscience Lab of Kyungpook National University, South Korea. After transportation the bats were immediately anesthetized with a mixture of ketamine hydrochloride (30-40 mg/kg) and xylazine (3-6 mg/kg) before perfusion. They were intracardially perfused with 4% paraformaldehyde and 0.3-0.5% glutaraldehyde in 0.1 M sodium phosphate buffer (pH 7.4) with 0.002% calcium chloride. Following a pre-rinse with phosphate-buffered saline (PBS; pH 7.4, 40 ml) over a 3-5 min period, each animal was perfused with a fixative (fix buffer, 30-50 ml) for 20-30 min via a syringe needle inserted through the left ventricle and aorta. The head was then removed and placed in the fixative for 2-3 h. The brain was then removed from the skull and stored for 2-3 h in the same fixative, and then stored overnight in PBS (pH 7.4) containing 0.002% $CaCl_2$. Blocks of visual cortex were cut and sectioned (50 μm) on the frontal plane with a Vibratome 3000 Plus Sectioning System (St. Louis, Missouri, USA). For every four or five sections, three or four sections were used for immunocytochemistry and one was used for thionin staining. The thionin-stained sections were used to identify cortical layers. The guidelines of the National Institutes of Health for the Care and Use of Laboratory Animals were followed for all experimental procedures.

Horseradish peroxidase (HRP) immunocytochemistry

Polyclonal antibodies against CR and PV were obtained from Chemicon International Inc. (Billerica, Massachusetts, USA). A Polyclonal antibody against CB was obtained from Sigma-Aldrich (St. Louis, Missouri, USA). The primary antiserum was diluted 1:500-1:1000 and the biotinylated secondary antiserum was diluted 1:200. Standard immunocytochemical techniques and methods were used, as described previously (Hong et al., 2002). The sections were examined and photographed on a Zeiss Axioplan microscope (Carl Zeiss Meditec Incorporation, Jena, Germany) with conventional or differential interference contrast (DIC) optics.

Fluorescence immunocytochemistry

A monoclonal antibody against GABA was obtained from Chemicon International Inc. (Billerica, Massachusetts, USA). Polyclonal antibodies against CB, CR, and PV were obtained from Sigma-Aldrich (St. Louis, Missouri, USA). To double-label CB-, CR-, and PV-IR-positive sections with GABA, sections were incubated in primary antiserum as described above. The primary antiserum was diluted either 1:250 (GABA), or 1:500-1:1000 (CB, CR, and PV). For CB, CR, and PV, the secondary antibodies were fluorescein (FITC)-conjugated anti-rabbit IgG (Vector Laboratories, Burlingame, California, USA). A Cy3-conjugated anti-mouse IgG (Jackson ImmuoResearch, West Grove, Pennsylvania, USA) secondary antibody was used to identify GABA. Labeled sections were preserved under cover slips in Vectashield mounting medium (Vector Laboratories). Images were obtained and viewed with a Zeiss LSM700 laser scanning confocal microscope (Carl Zeiss Meditec Incorporation).

Quantitative analysis

The areas of CB-, CR-, and PV-IR neurons were computed using a digital camera, Zeiss AxioCam HRc (AxioVision 4; Carl Zeiss Meditec Incorporation) with a 20× objective. Double-labeled neurons were counted in nine different sections, each 1,500 μm in width, from all layers. Double-labeled images were obtained on a Zeiss LSM700 laser scanning confocal microscope (Carl Zeiss Meditec Incorporation) using a 40× objective. The morphological types of CB-, CR-, and PV-IR neurons were analyzed in DAB-reacted sections. All analyses were done with a 40× Zeiss Plan-Apochromat objective. To obtain the best images, we analyzed cells under DIC optics. Only cell profiles containing a nucleus and at least a faintly visible nucleolus were included in this analysis. Since our goal was to obtain an estimate of each morphological cell type, no attempt was made to assess the total number of cells in each neuronal subpopulation. In Figs. 5, 6, we used the ANOVA via the Statistical Package for the Social Science (SPSS; International Business Machines Corporation, Armonk, New York, USA) to identify each CBP-IR neurons' distribution in the highest level of density.

Results

The distribution of CBP-IR neurons

Each type of CBP-IR neuron (i.e., CB-, CR-, and PV-IR) was selectively distributed in the bat visual cortex (Figs. 1, 5). The highest density of CB-IR neurons was located in layer IV. Layer IV shows a significant difference among the other layers (p value < 0.05). The frequency of CB-IR neurons varied in each layer: 1.44% (0.56 cells on average) of labeled neurons were found in layer I, 15.25% (5.87 cells on average) in layer II, 16.69% (6.43 cells on average) in layer III, 33.23% (12.78 cells on average) in layer IV, 21.03% (8.10 cells on average) in layer V, and 12.36% (4.76 cells on average) in layer VI. CR-IR neurons were predominantly located in layers II/III. Significantly lower densities of these neurons were observed in other layers (p value < 0.05). A quantitative histogram of cell distribution

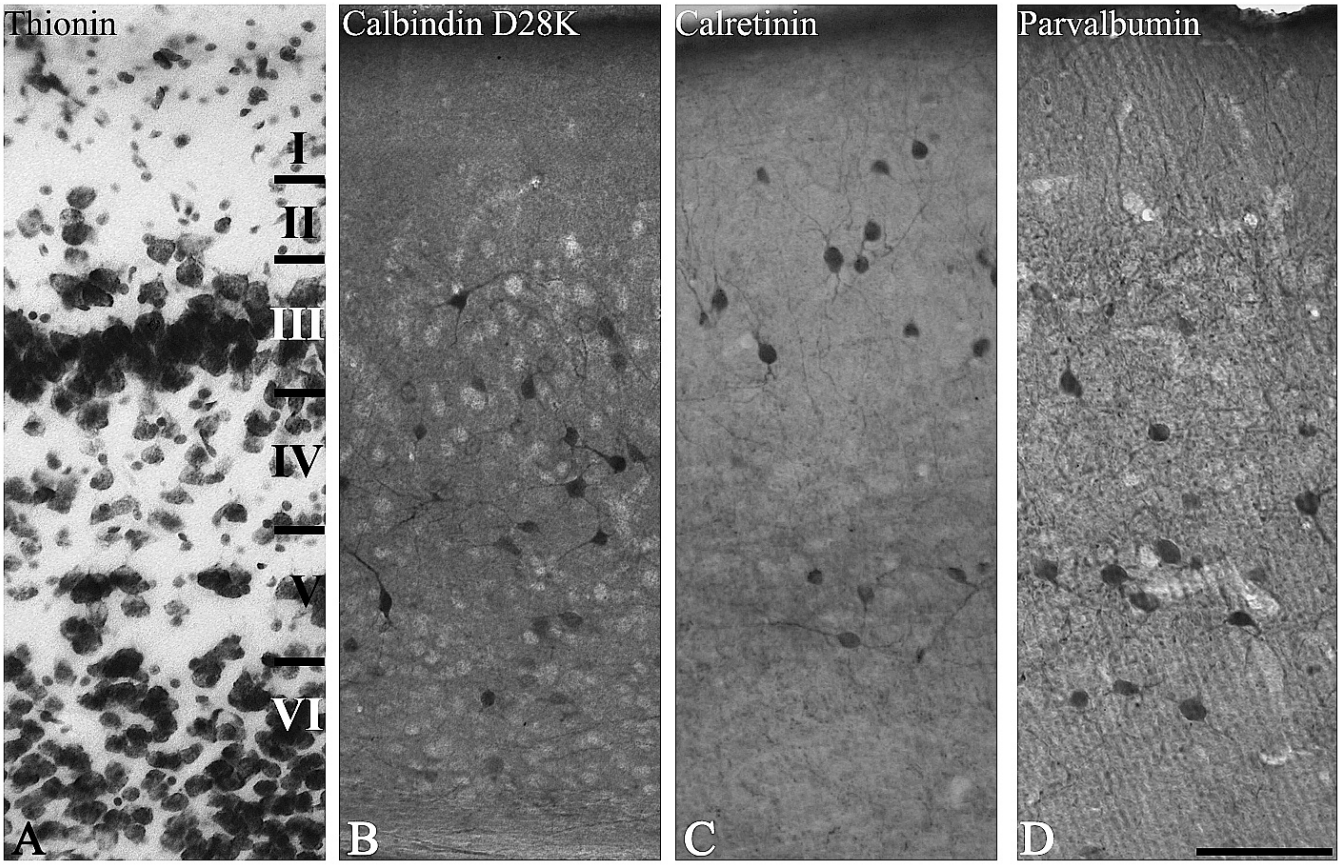

Fig. 1. Low-power photomicrographs of the calbindin D28K (CB)-, calretinin (CR)-, and parvalbumin (PV)-immunoreactive (IR) neuron distribution in the bat visual cortex. **A.** A thionin-stained section illustrating cortical lamination. **B.** CB-IR neurons. **C.** CR-IR neurons. **D.** PV-IR neurons. CB-, CR-, and PV-IR neurons were selectively distributed in many cells. Scale bar: 100 μm.

revealed the density of CR-IR neurons in each layer (Fig. 5): 8.51% (4.44 cells on average) of labeled neurons were found in layer I, 58.59% (30.63 cells on average) in layer II, 22.47% (11.75 cells on average) in layer III, 6.74% (3.57 cells on average) in layer IV, 2.41% (1.19 cells on average) in layer V, and 1.28% (0.63 cells on average) in layer VI. The highest density of PV-IR neurons was located in layer IV. Layer IV shows a significant difference among the other layers (p value <0.05). A quantitative histogram of cell distribution revealed the density of the PV-IR neurons in each layer (Fig. 5): 3.53% (1.11 cells on average) of labeled neurons were found in layer I, 19.90% (6.19 cells on average) in layer II, 15.57% (4.84 cells on average) in layer III, 39.33% (12.30 cells on average) in layer IV, 19.90% (6.19 cells on average) in layer V, and

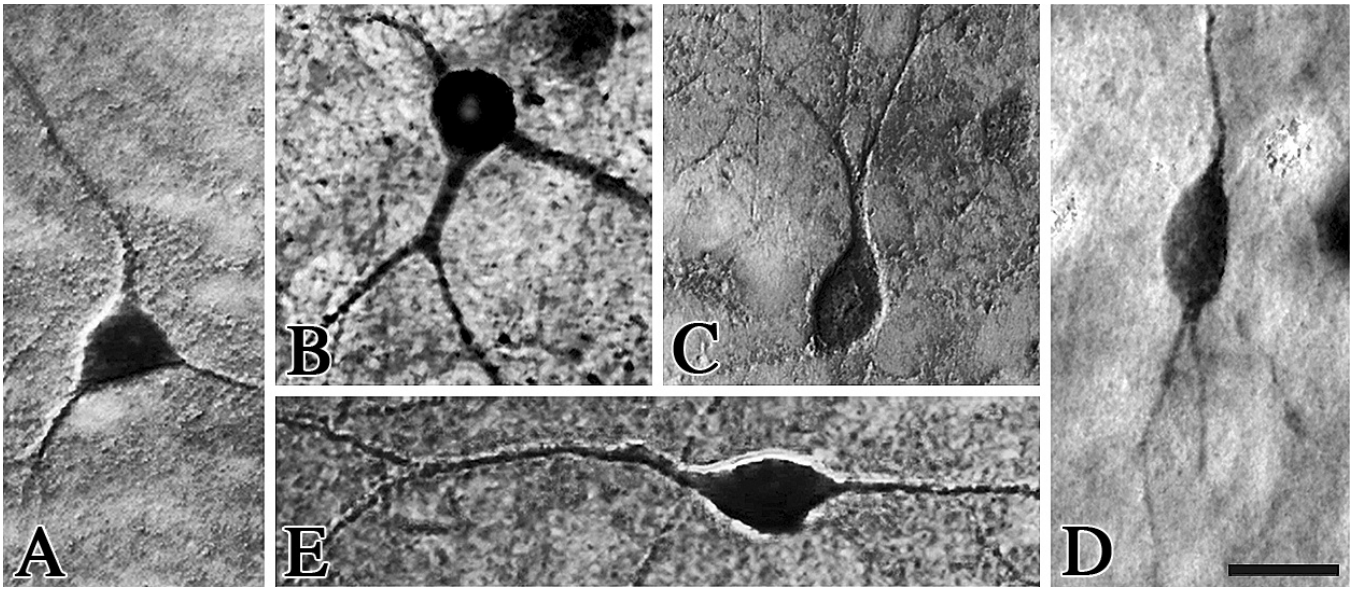

Fig. 2. High-power differential interference contrast (DIC) photomicrographs of CB-IR neurons in the bat visual cortex. **A.** Multipolar stellate type with a polygonally shaped cell body. **B.** Multipolar round type. **C.** Pyriform type with a dendrite directed towards the pial surface. **D.** Vertical fusiform type with a vertical fusiform cell body and vertically oriented processes. **E.** Horizontal fusiform type with a horizontal fusiform cell body and horizontally oriented processes. Scale bar: 20 µm.

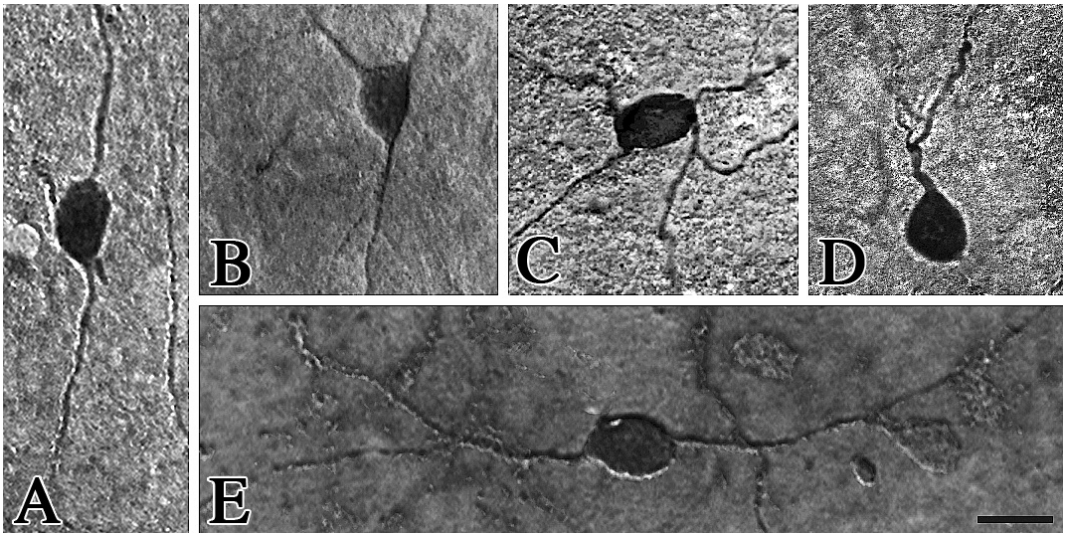

Fig. 3. DIC photomicrographs of CR-IR neurons in the bat visual cortex. **A.** Vertical fusiform type with a vertical fusiform cell body and vertically oriented processes. **B.** Multipolar stellate type with a polygonally shaped cell body. **C.** Multipolar oval type. **D.** Pyriform type with a pyriform cell body and a dendrite directed towards the pial surface. **E.** Horizontal type with a horizontal fusiform cell body with horizontally oriented processes. Scale bar: 20 µm.

1.77% (0.56 cells on average) in layer VI.

Morphology of CB-IR neurons in the bat visual cortex

CB-IR neurons varied in shape in the bat visual cortex: multipolar stellate, multipolar round/oval, vertical fusiform, horizontal, and pyriform (Fig. 6). The majority of CB-IR neurons in the bat visual cortex were stellate or round/oval. The p value of CB-IR neuron with round/oval and stellate shape shows less than 0.05, and it was defined as being statistically significant. Fig. 2B shows a representative multipolar round/oval type, which had a round/oval cell body and many dendrites coursing in all directions. Fig. 2A shows a stellate type, which had a polygonal-shaped cell body and many dendrites coursing in all directions. Fig. 2C shows a pyriform type, which had a pyriform cell body and thick, proximal dendrites directed toward the pial surface. Fig. 2D shows a vertical fusiform type, which had a vertical fusiform cell body with a long main process ascending toward the pial surface, as well as a descending process. Fig. 4E shows a horizontal type, which had a horizontally oriented cell body and dendrites. Quantitatively, 28.66% (135 of 471 cells) of CB-IR neurons were multipolar stellate type, 56.69% (267 of 471 cells) were multipolar round/oval type, 9.34% (44 of 471 cells) were vertical fusiform type, 3.61% (17 of 471 cells) were horizontal type, and 1.70% (8 of 471 cells) were pyriform type (Fig. 6).

Morphology of CR-IR neurons in the bat visual cortex

CR-IR neurons consisted of various shapes in the bat visual cortex. The majority of CR-IR neurons were multipolar round/oval type with dendrites oriented from the perikaryon, reaching out in all directions (Figs. 3C, 6). The p value of CR-IR neuron with multipolar round/oval type shows less than 0.05, and it was defined as being statistically significant. Fig. 3A shows a vertical fusiform type, which had a long main process ascending towards the pial surface, as well as a descending process. The stellate type also had several dendrites oriented in various directions (Fig. 3B). Fig. 3D shows a pyriform type, which had a thick primary dendrite directed toward the pial surface. A horizontal type (Fig. 3E), which had a horizontal fusiform cell body and horizontally-oriented processes, also contained CR. Quantitatively, 14.41% (50 of 347 cells) of CB-IR neurons were multipolar round/oval type, 48.99% (170 of 347 cells) were multipolar stellate type, 30.84% (107 of 347 cells) were vertical fusiform type, 3.17% (11 of 347 cells) were horizontal type, and 2.59% (9 of 347 cells) were pyriform type (Fig. 6).

Morphology of PV-IR neurons in the bat visual cortex

The morphology of PV-IR neurons also varied and was quite different from that of CB- and CR-IR neurons (Fig. 6). The majority of PV-IR neurons were multipolar stellate type with many dendritic processes in all directions (Figs. 3D, 6). The p value of PV-IR neuron with multipolar stellate type shows less than 0.05, and it was defined as being statistically significant. Fig. 4A shows a pyriform type, which had a pyriform cell body with a thick and proximal dendrite directed towards the pial surface; this type of PV-IR neuron was rarely

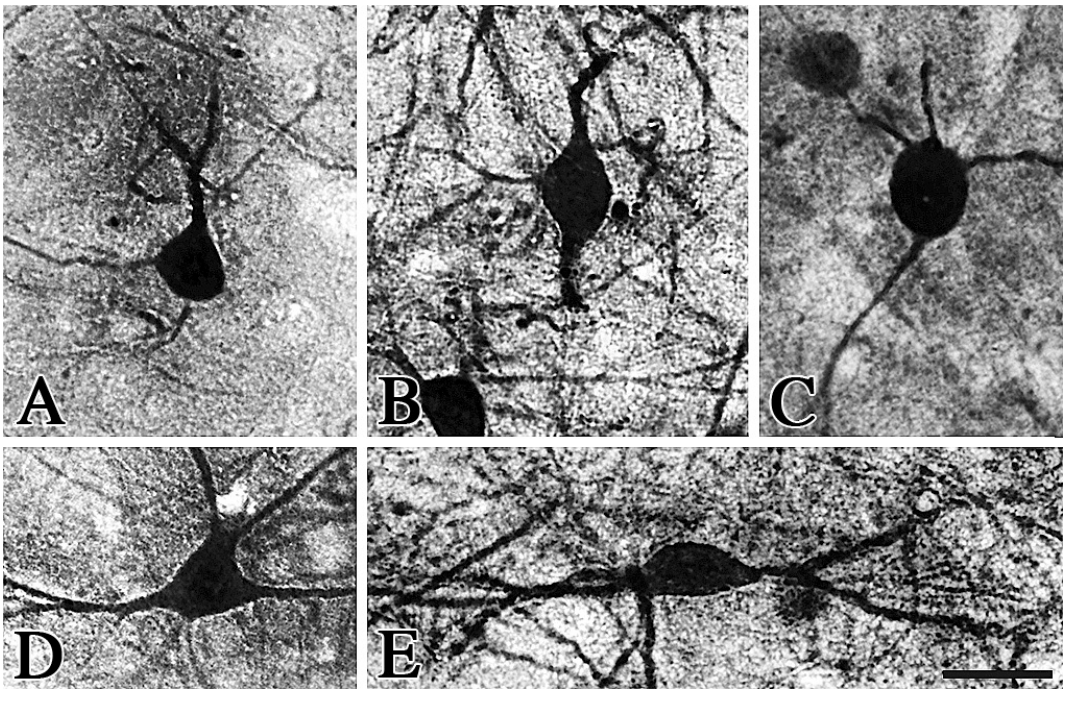

Fig. 4. DIC photomicrographs of PV-IR neurons in the bat visual cortex. **A.** Pyriform type with a pyriform cell body and a thick dendrite directed towards the pial surface. **B.** Vertical fusiform type. **C.** Multipolar round type. **D.** Multipolar stellate type with a polygonally shaped cell body. **E.** Horizontal type with a horizontal fusiform cell body with horizontally oriented processes. Scale bar: 20 µm.

observed in the bat visual cortex. Fig. 4B,C shows a vertical fusiform type and a multipolar round/oval type, respectively. The vertical fusiform type had a vertical fusiform cell body with a thick proximal vertical dendrite directed toward the pial surface. The round/oval type had round/oval cell bodies with several dendrites coursing in various directions. The horizontal type (Fig. 4E) with horizontally oriented processes also contained PV. Quantitatively, 50.35% (142 of 282 cells) of PV-IR neurons were multipolar stellate type, 31.91% (90 of 282 cells) were multipolar round/oval type, 9.57% (27 of 282 cells) were vertical fusiform type, 7.09% (20 of 282 cells) were horizontal type, and 1.06% (3 of 282 cells) were pyriform type (Fig. 6).

Co-localization of CBPs and GABA

To determine whether CB-, CR-, and PV-IR neurons in the visual cortex co-localized with GABA, we labeled CBPs with FITC and GABA with Cy3. Some neurons were clearly labeled by anti-GABA and anti-calbindin D28K, anti-calretinin, or anti-parvalbumin antibodies in the bat visual cortex. Other neurons were only labeled by a single antibody, but not both (Figs. 7, 8, Table 1). Arrowheads in Fig. 8C,F,I show CBP and GABA double-labeled neurons. To estimate the percentage of double-labeled neurons, we counted the number of CBP-IR neurons and double-labeled neurons across the layers of the bat visual cortex in nine sections from three animals. Quantitatively, 65.96±15.95% (mean ± standard deviation [S.D.]) of CB-IR neurons were double-labeled with GABA. In the case of CR-IR neurons, 24.24±9.02% of neurons were double-labeled with GABA. In the case of PV-IR neurons, 77.00±13.41% of neurons were double-labeled with GABA (Table 1). This percentage of double-labeled neurons was relatively consistent across sections and among animals.

Discussion

Our study showed that CB-, CR-, and PV-IR neurons were distributed in specific layers of the bat visual cortex. The highest density of CB-IR neurons in the bat visual cortex was found in layer IV. The distribution pattern of CB-IR neurons in bat visual cortex, however, was significantly different from previously studied animals. For instance, CB-IR neurons in the visual cortex of rat (Gonchar and Burkhalter, 1997), mouse (Park et al., 2002), and rabbit (Park et al., 2000) were found at highest density in layer V. In addition, in human (Leuba and Saini, 1996), monkey (Hendrickson et al., 1991; Goodchild and Martin, 1998), flying fox (Ichida et al., 2000), and cat (Stichel et al., 1987) the highest density of CB-IR neurons was found in layer II/III. Unlike CB-IR neurons, the distribution pattern of CR-IR

Table 1. Percentage of neurons double-labeled with calcium binding proteins (CBPs) and GABA in the bat visual cortex.

Antibody	No. of Sections	No. of Cells	No. of Double	% Double (Means ± S.D.)
Calbindin D28K	9	94	62	65.96±15.95
Calretinin	9	66	16	24.24±9.02
Parvalbumin	9	100	77	77.00±13.41

S.D., standard deviation.

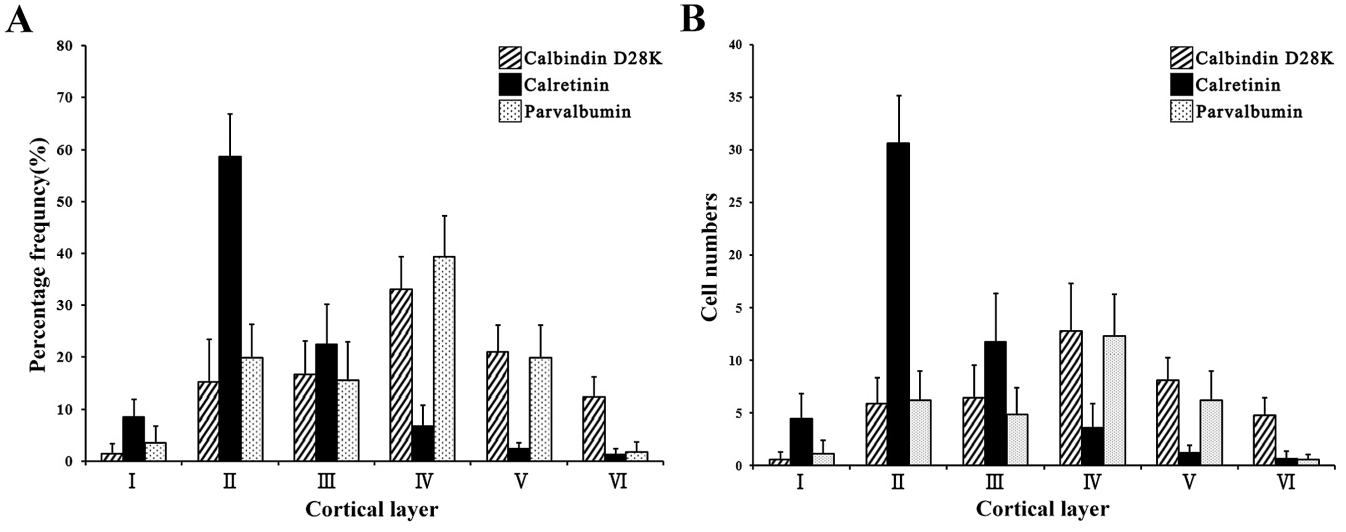

Fig. 5. Histogram of the distribution of neurons labeled by CB, CR, and PV antibodies in the bat visual cortex. The highest density of CB-IR neurons was located in layer IV. CR-IR neurons were mostly located in layers II/III, while PV-IR neurons were predominantly located in layer IV.

neurons in the bat visual cortex was similar to those of many mammals. In the present study, CR-IR neurons were predominantly located in layers II/III. Similarly, the highest density of CR-IR neurons in the human (Glezer et al., 1992), monkey (Meskenaite, 1997), hamster (Lee et al., 2004), rabbit (Park et al., 1999), rat (Gonchar and Burkhalter, 1997), and cat (Jeon and Park, 1997) visual cortex were also located in layer II/III. The laminar position of PV-IR neurons varies slightly among species. In the present study, the highest density of PV-IR neurons was observed in layer IV. Similar to our data, in the human (Leuba and Saini, 1996), monkey (Hendrickson et al., 1991), and cat (Demeulemeester et al., 1991) visual cortex, the highest density of PV-IR neurons was located in layer IV. However, PV-IR neurons in the visual cortex of the new world monkey and marmoset (Goodchild and Martin, 1998) were mostly located in layers II-VI, PV-IR neurons were not observed in layer I. In rabbit visual cortex PV-IR neurons were mainly located in layers III-VI (Park et al., 2000). In the mouse and hamster visual cortex, PV-IR

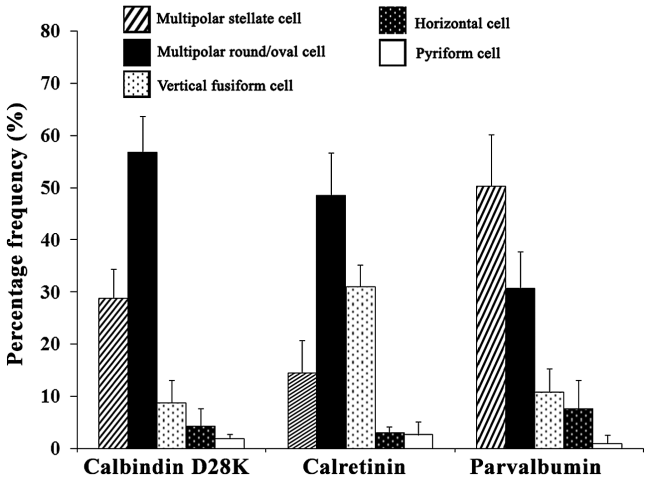

Fig. 6. Histogram of the distribution of morphologically different types of neurons labeled by CB, CR, and PV in the bat visual cortex. The majority of CB- and CR-IR neurons are multipolar round/oval types, while many PV-IR neurons are multipolar stellate type.

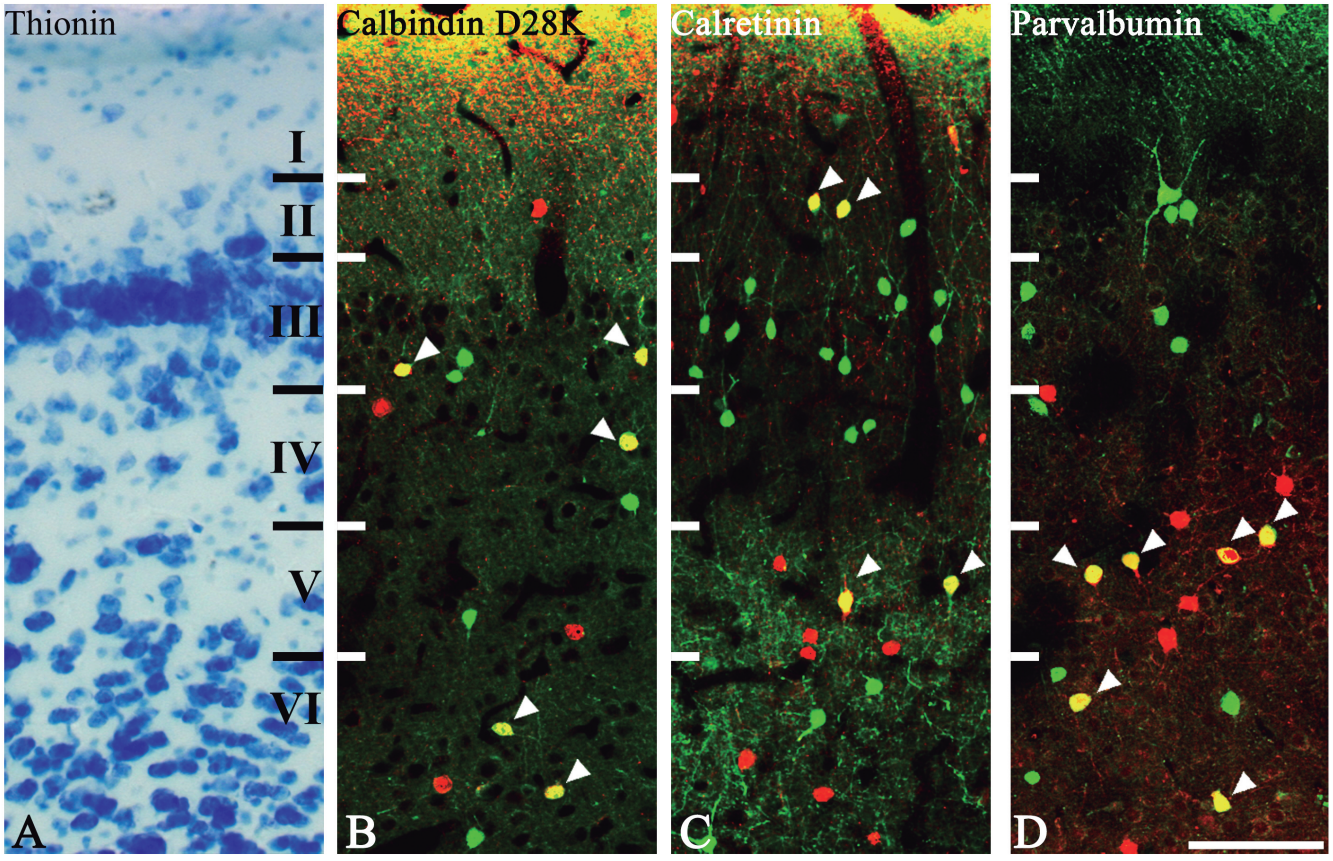

Fig. 7. Low magnification fluorescence confocal photomicrographs showing the cortical distribution of CBPs and GABA in the bat visual cortex. **A.** A thionin-stained section illustrating cortical lamination. **B.** Superimposition of CB (green)- and GABA (red)-positive images. Arrowheads indicate double-labeled neurons. **C.** Superimposition of CR (green)- and GABA (red)-positive images. Arrowheads indicate double-labeled neurons. **D.** Superimposition of PV (green)- and GABA (red)-positive images. Arrowheads indicate double-labeled neurons. Scale bar: 100 μm.

neurons were mainly located in layers IV-VI (Park et al., 1999). The functional role of different laminar distributions of these CBPs among species is not yet understood. However, the different laminar segregation of these proteins among species may reveal the subtle functional segregation of these proteins in visual processing.

The major types of CB-IR neurons in bat visual

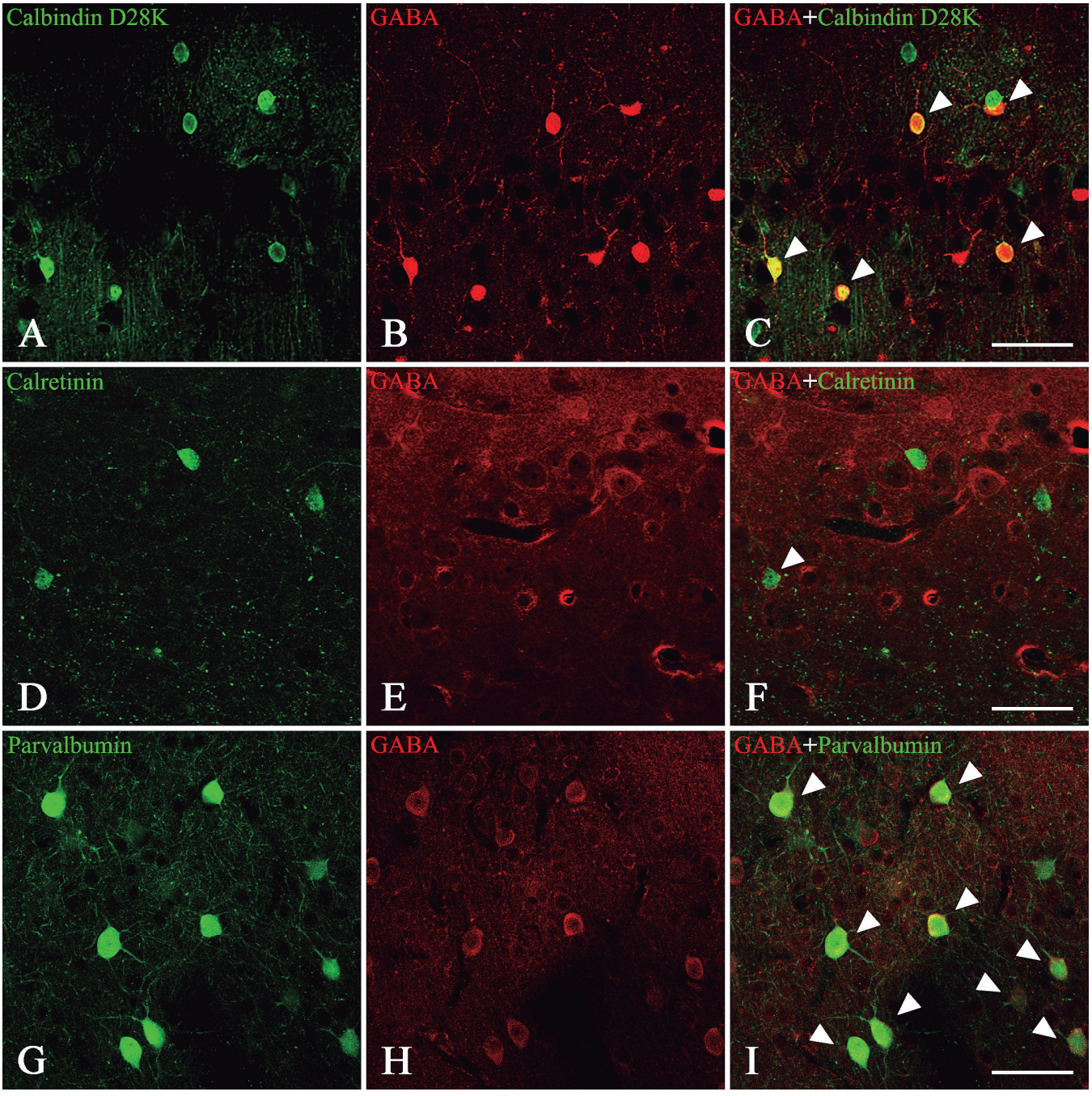

Fig. 8. Medium magnification of fluorescence confocal photomicrographs immunostained for CB **(A),** CR **(D)**, PV **(G)**, and gamma-aminobutyric acid (GABA) **(B, E, and H)** in the bat visual cortex. **C.** Superimposition of CB- and GABA-positive images. Arrowheads indicate double-labeled neurons. **F.** Superimposition of CR- and GABA-positive images. The arrowhead indicates a double-labeled neuron. **I.** Superimposition of PV- and GABA-positive images. Arrowheads indicate double-labeled neurons. Scale bar: 50 µm.

cortex were multipolar stellate and round/oval in shape. In the present study, a few fusiform, horizontal, and pyriform neurons were also labeled by the anti-CB antibody. The types of CB-IR neurons found in the bat visual cortex were similar to those identified in the visual cortex of other animals, such as humans (Leuba and Saini, 1996), monkeys (Hendrickson et al., 1991), cats (Stichel et al., 1987), rats (Gonchar and Burkhalter, 1997), flying foxes (Ichida et al., 2000) and hamsters (Lee et al., 2004). The types of CR-IR neurons identified in the bat visual cortex were similar to those identified in the visual cortex of humans (Glezer et al., 1992), dolphins (Glezer et al., 1992), dogs (Yu et al., 2011), monkeys (Hendrickson et al., 1991), cats (Jeon and Park, 1997), rats (Gonchar and Burkhalter, 1997), and hamsters (Lee et al., 2004). In all of these species, the majority of CR-IR neurons were the vertical fusiform type, which had a vertical fusiform cell body with a long main process ascending towards the pial surface, as well as a descending process. Similarly, the majority of CR-IR neurons in the bat were multipolar round/oval and vertical fusiform in shape. The types of PV-IR neurons in bat visual cortex were similar to those identified in the human (Blümcke et al., 1990; Leuba and Saini, 1996), monkey (Blümcke et al., 1990; Hendrickson et al., 1991), cat (Stichel et al., 1987; Demeulemeester et al., 1991), rat (Gonchar and Burkhalter, 1997), rabbit (Park et al., 2000), mouse and hamster (Park et al., 1999) visual cortex. In all these species, the majority of PV-IR neurons were multipolar stellate and round/oval in shape. A small number of horizontal, pyriform, and vertical fusiform cells also contained PV. The results of these studies indicated that CBP-IR neuron morphologies in the bat visual cortex were in accordance with previous findings in most mammals. This suggested that the functional role of the CBP-IR neurons in bat visual cortex did not significantly differ from other mammals.

The morphological properties of CB-, CR-, and PV-IR neurons in the bat visual cortex suggested that many of these neurons were interneurons. The present study demonstrated that CB-, CR-, and PV-IR neurons in the bat visual cortex were labeled by GABA (65.96%, 24.24%, and 77.00%, respectively). Similarly, in the cat visual cortex (Demeulemeester et al., 1991), approximately 80% of CB-IR neurons were labeled by GABA. In the rat visual cortex (Gonchar and Burkhalter, 1997), 97% of CB-IR neurons, 94% of CR-IR neurons, and of 100% PV-IR neurons were also labeled by GABA. In the monkey visual cortex (Meskenaite, 1997), approximately 95% of CR-IR neurons were GABAergic interneurons. In the dog visual cortex (Yu et al., 2011), 66% of CB-IR neurons, 91% of CR-IR neurons, and 96% of PV-IR neurons were also labeled by GABA. Although the number of double-labeled neurons in the bat visual cortex was generally lower than that in previously studied animals, these results indicated that many of the CBP-IR neurons in the bat visual cortex were GABAergic interneurons.

The functional role of CBPs in the CNS is not yet understood. However, it is generally known that CBPs are involved in buffering the intracellular calcium level to maintain cellular homeostasis (Baimbridge et al., 1992; Chard et al., 1993). Recent studies showed that CB was involved in signaling pathways that modulate behavioral and molecular responses to light (Stadler et al., 2010). CR modulated voltage-gated calcium channels (Christel et al., 2012). PV was involved in regulating information processing in the central visual pathway (Lintas et al., 2013). In addition, CBPs are closely related to neurological disorders and age in the visual cortex. For example, CB- and CR-IR neurons decreased in association with age in the primary visual cortex (Bu et al., 2003). However, there was no significant decrease in CB-, CR-, or PV-IR neurons in the visual cortex of Alzheimer's disease patients (Leuba et al., 1998). In contrast, the density of CB-GABA double-labeled neurons in the visual cortex of depressive disorder patients was reduced (Maciag et al., 2010). All these data suggested that CBP-IR neurons in the visual cortex play important roles in various functions.

Visual evoked potential (VEP) or behavior tests have not been executed yet in bat. In previous studies, however, it has been revealed that VC of mouse (Ridder and Nusinowitz, 2006), rat (Brankack et al., 1990), cat (Padnick and Linsenmeier, 1999), monkey and human (Lamme et al., 1992) is associated with visual functions such as responses to illumination and determination of visual textures through VEP test. Recent results showed that the primary visual cortex is required for discriminating complex images, direction and motion in rat (Petruno et al., 2013), and perceiving changes in the direction and the contrast of the target in mouse (Glickfeld et al., 2013). These data along with the fact that CBPs exist in almost the same subpopulation of neurons in many vertebrate visual cortical neurons including bats indicate that bats might have visual abilities. However, more data need to be added to confirm the visual cortical functions in bat.

In conclusion, our study showed that CB-, CR-, and PV-IR neurons were present in specific layers of the bat visual cortex. The large majority of CB- and CR-IR neurons were round/oval in shape, while the majority of PV-IR neurons were stellate. Double-labeling experiments with GABA suggested that many of the CBP-IR neurons were GABAergic interneurons. The present study should aid in a better understanding of the bat visual system.

Acknowledgements. We thank Cactus Communications for proofreading the manuscript. This research was supported by Basic Science Research Program through the National Research Foundation of Korea (NRF) funded by Ministry of Education (NRF-2013R1A1A2059568).

References

Alexianu M.E., Ho B.K., Mohamed A.H., La Bella V., Smith R.G. and

Appel S.H. (1994). The role of calcium-binding proteins in selective motoneuron vulnerability in amyotrophic lateral sclerosis. Ann. Neurol. 36, 846-858.

Baimbridge K.G., Celio M.R. and Rogers J.H. (1992). Calcium-binding proteins in the nervous system. Trends Neurosci. 15, 303-308.

Blümcke I., Hof P.R., Morrison J.H. and Celio M.R. (1990). Distribution of parvalbumin immunoreactivity in the visual cortex of Old World monkeys and humans. J. Comp. Neurol. 30, 417-432.

Bu J., Sathyendra V., Nagykery N. and Geula C. (2003). Age-related changes in calbindin-D28k, calretinin, and parvalbumin-immunoreactive neurons in the human cerebral cortex. Exp. Neurol. 182, 220-231.

Brankack J., Schober W. and Klingberg F. (1990). Different laminar distribution of flash evoked potentials in cortical areas 17 and 18 b of freely moving rats. J. Hirnforsch. 31, 525-533.

Chard P.S., Bleakman D., Christakos S., Fullmer C.S. and Miller R.J. (1993). Calcium buffering properties of calbindin D28k and parvalbumin in rat sensory neurons. J. Physiol. 472, 341-357.

Christel C.J., Schaer R., Wang S., Henzi T., Kreiner L., Grabs D., Schwaller B. and Lee A. (2012). Calretinin regulates Ca2+-dependent inactivation and facilitation of Ca(v)2.1 Ca2+ channels through a direct interaction with the α12.1 subunit. J. Biol. Chem. 287, 39766-39775.

Demeulemeester H., Arckens L., Vandesande F., Orban G.A., Heizmann C.W. and Pochet R. (1991). Calcium binding proteins and neuropeptides as molecular markers of GABAergic interneurons in the cat visual cortex. Brain Res. 84, 538-544.

Ellis J.H., Richards D.E. and Rogers J.H. (1991). Calretinin and calbindin in the retina of the developing chick. Cell Tissue Res. 264, 197-208.

Gao W.J., Wormington A.B., Newman D.E. and Pallas S.L. (2000). Calcium-binding proteins calbindin D28K, calretinin, and parvalbumin immunoreactivity in the rabbit visual cortex. J. Comp. Neurol. 422, 140-157.

Glezer I.I., Hof P.R. and Morgane P.J. (1992). Calretinin-immunoreactive neurons in the primary visual cortex of dolphin and human brains. Brain Res. 595, 181-188.

Glezer I.I., Hof P.R. and Morgane P.J. (1998). Comparative analysis of calcium-binding protein-immunoreactive neuronal populations in the auditory and visual systems of the bottlenose dolphin (*Tursiops truncatus*) and the macaque monkey (*Macaca fascicularis*). J. Chem. Neuroanat. 15, 203-237.

Glickfeld L.L., Histed M.H. and Maunsell J.H. (2013). Mouse primary visual cortex is used to detect both orientation and contrast changes. J. Neurosci. 33, 19416-19422.

Gonchar Y. and Burkhalter A. (1997). Three distinct families of GABAergic neurons in rat visual cortex. Cereb. Cortex 7, 347-358.

Goodchild A.K. and Martin P.R. (1998). The distribution of calcium-binding proteins in the lateral geniculate nucleus and visual cortex of a New World monkey, the marmoset, *Callithrix jacchus*. Vis. Neurosci. 15, 625-642.

Gutierrez Ede A., Pessoa V.F., Aguiar L.M. and Pessoa D.M. (2014). Effect of light intensity on food detection in captive great fruit-eating bats, Artibeus lituratus (Chiroptera: Phyllostomidae). Behav. Processes 109, 64-69.

Hage S.R. and Metzner W. (2013). Potential effects of anthropogenic noise on echolocation behavior in horseshoe bats. Commun. Integr. Biol. 6, e24753.

Heizmann C.W. (1984). Parvalbumin, an intracellular calcium-binding protein; distribution, properties and possible roles in mammalian cells. Experientia 40, 910-921.

Heizmann C.W., Röhrenbeck J. and Kamphuis W. (1990). Parvalbumin, molecular and functional aspects. Adv. Exp. Med. Biol. 269, 57-66.

Hendrickson A.E., Van Brederode J.F., Mulligan K.A. and Celio M.R. (1991). Development of the calcium-binding protein parvalbumin and calbindin in monkey striate cortex. J. Comp. Neurol. 307, 626-646.

Holland R.A., Waters D.A. and Rayner J.M. (2004). Echolocation signal structure in the Megachiropteran bat Rousettus aegyptiacus Geoffroy 1810. J. Exp. Biol. 207, 4361-4369.

Hong S.K., Kim J.Y. and Jeon C.J. (2002). Immunocytochemical localization of calretinin in the superficial layers of the cat superior colliculus. Neurosci. Res. 44, 325-335.

Ichida J.M., Rosa M.G. and Casagrande V.A. (2000). Does the visual system of the flying fox resemble that of primates? The distribution of calcium-binding proteins in the primary visual pathway of Pteropus poliocephalus. J. Comp. Neurol. 417, 73-87.

Jeon C.J. and Park H.J. (1997). Immunocytochemical localization of calcium-binding protein calretinin containing neurons in cat visual cortex. Mol. Cells 7, 721-725.

Jeon Y.K., Kim T.J., Lee J.Y., Choi J.S. and Jeon C.J. (2007). AII amacrine cells in the inner nuclear layer of bat retina: identification by parvalbumin immunoreactivity. Neuroreport 18, 1095-1099.

Jeong S.J., Kim H.H., Lee W.S. and Jeon C.J. (2014). Immunocytochemical Localization of Calbindin D28K, Calretinin, and Parvalbumin in Bat Superior Colliculus. Acta. Histochem. Cytochem. 47, 113-123.

Jones G. and Rayner J.M.V. (1989). Foraging behavior and echolocation of wild horseshoe bats Rhinolophus ferrumequinum and R. hipposideros (Chiroptera, Rhinolophidae). Behav. Ecol. Sociobiol. 25, 183-191.

Kim T.J., Jeon Y.K., Lee J.Y., Lee E.S. and Jeon C.J. (2008). The photoreceptor populations in the retina of the greater horseshoe bat Rhinolophus ferrumequinum. Mol. Cells 26, 373-379.

Lamme V.A., Van Dijk B.W. and Spekreijse H. (1992). Texture segregation is processed by primary visual cortex in man and monkey. Evidence from VEP experiments. Vision Res. 32, 797-807.

Lee J.E., Ahn C.H., Lee J.Y., Chung E.S. and Jeon C.J. (2004). Nitric oxide synthase and calcium-binding protein-containing neurons in the hamster visual cortex. Mol. Cells 18, 30-39.

Leuba G. and Saini K. (1996). Calcium-binding proteins immunoreactivity in the human subcortical and cortical visual structures. Vis. Neurosci. 13, 997-1009.

Leuba G., Kraftsik R. and Saini K. (1998). Quantitative distribution of parvalbumin, calretinin, and calbindin D-28k immunoreactive neurons in the visual cortex of normal and Alzheimer cases. Exp. Neurol. 152, 278-291.

Lintas A., Schwaller B. and Villa A.E. (2013). Visual thalamocortical circuits in parvalbumin-deficient mice. Brain Res. 1536, 107-118.

Maciag D., Hughes J., O'Dwyer G., Pride Y., Stockmeier C.A., Sanacora G. and Rajkowska G. (2010). Reduced density of calbindin immunoreactive GABAergic neurons in the occipital cortex in major depression: relevance to neuroimaging studies. Biol. Psychiatry 67, 465-470.

Meskenaite V. (1997). Calretinin-immunoreactive local circuit neurons in area 17 of the cynomolgus monkey, *Macaca fascicularis*. J. Comp. Neurol. 379, 113-132.

Neuweiler G. (1990). Auditory adaptation for prey capture in echolocating bats. Physiol. Rev. 70, 615-641.

Padnick L.B. and Linsenmeier R.A. (1999). Properties of the flash visual evoked potential recorded in the cat primary visual cortex. Vision Res. 39, 2833-2840.

Park H.J., Hong S.K., Kong J.H. and Jeon C.J. (1999). Localization of calcium-binding protein parvalbumin-immunoreactive neurons in mouse and hamster visual cortex. Mol. Cells 9, 542-547.

Park H.J., Lee S.N., Lim H.R., Kong J.H. and Jeon C.J. (2000). Calcium-binding proteins calbindin D28K, calretinin, and parvalbumin immunoreactivity in the rabbit visual cortex. Mol. Cells 10, 206-212.

Park H.J., Kong J.H., Kang Y.S., Park S.M., Lim J.K. and Jeon C.J. (2002). The distribution and morphology of calbindin D28K- and calretinin-immunoreactive neurons in the visual cortex of mouse. Mol. Cells 14, 143-149.

Petruno S.K., Clark R.E. and Reinagel P. (2013). Evidence that primary visual cortex is required for image, orientation, and motion discrimination by rats. PLoS One 8, e56543

Ridder W.H. 3rd. and Nusinowitz S. (2006). The visual evoked potential in the mouse-origins and response characteristics. Vision Res. 46, 902-913.

Rogers J.H. (1987). Calretinin: a gene for a novel calcium binding protein expressed principally in neurons. J. Cell Biol. 105, 1343-1353.

Schäfer B.W. and Heizmann C.W. (1996). The S100 family of EF-hand calcium-binding proteins: functions and pathology. Trends Biochem. Sci. 21, 134-140.

Simmons J.A. (1973). The resolution of target range by echolocating bats. J. Acoust. Soc. Am. 54, 157-173.

Stadler F., Schmutz I., Schwaller B. and Albrecht U. (2010). Lack of calbindin-D28k alters response of the murine circadian clock to light. Chronobiol. Int. 27, 68-82.

Stichel C.C., Singer W., Heizmann C.W. and Norman A.W. (1987). Immunohistochemical localization of calcium-binding proteins, parvalbumin and calbindin-D 28k, in the adult and developing visual cortex of cats: a light and electron microscopic study. J. Comp. Neurol. 262, 563-577.

Surlykke A., Boel Pedersen S. and Jakobsen L. (2009). Echolocating bats emit a highly directional sonar sound beam in the field. Proc. Biol. Sci. 276, 853-860.

Suthers R.A. (1970a). A comment on the role of choroidal papillae in the fruit bat retina. Vision Res. 10, 921-923.

Suthers R.A. and Wallis N.E. (1970b). Optics of the eyes of echolocating bats. Vision Res. 10, 1165-1173.

Vaughan T.A. and Vaughan R.P. (1986). Seasonality and the behavior of the African yellow-winged bat. J. Mammal. 67, 91-102.

Welsh M.J. (1988). Localization of intracellular calcium-binding proteins. In: Calcium binding proteins. Thompson M.P. (ed). CRC Press, Cleveland, Ohio, pp 1-19.

Winter Y., López J. and Von Helversen O. (2003). Ultraviolet vision in a bat. Nature 425, 612-614.

Xuan F., Hu K., Zhu T., Racey P., Wang X., Zhang S. and Sun Y. (2012). Immunohistochemical evidence of cone-based ultraviolet vision in divergent bat species and implication for its evolution. Comp. Biochem. Physiol. B, Biochem. Mol. Biol. 161, 398-403.

Yu S.H., Lee J.Y. and Jeon C.J. (2011). Immunocytochemical localization of calcium-binding proteins, calbindin D28K-, calretinin-, and parvalbumin-containing neurons in the dog visual cortex. Zool. Sci. 28, 694-702.

Zhao H., Xu D., Zhou Y., Flanders J. and Zhang S. (2009). Evolution of opsin genes reveals a functional role of vision in the echolocating little brown bat (Myotis lucifugus). Biochem. Syst. Ecol. 37, 154-161.

Accepted November 4, 2015